J. COMBIN. MATH. COMBIN. COMPUT. 127b (2025) 7879--7898

Journal of Combinatorial Mathematics and Combinatorial Computing
www.combinatorialpress.com/jcmcc

Combinatorial Press

Construction and analysis of digital intelligent flexible wrist rehabilitation equipment

Peijie Liu[1], Yushi Hu[1,✉]

[1] *School of Sports Medicine and Health, Chengdu Sport University, Chengdu, Sichuan, 641419, China*

ABSTRACT

In order to promote the development of medical rehabilitation industry, the study deeply analyzes flexible wearable devices and utilizes joint moment estimation based on skeletal muscle model in order to calculate the joint moments of elbow and wrist joints, so as to carry out the design of flexible pneumatic wrist joint system. And a fuzzy-PI dual-mode control strategy is used in the position control of the flexible pneumatic wrist joint to construct an intelligent flexible rehabilitation device for the wrist joint. The wrist joint rehabilitation equipment is systematically tested to analyze its practical application effect. The response speed of the fuzzy-PI dual-mode control method is faster than that of the traditional PID control strategy, and it can effectively reduce the vibration noise. The accuracy of the hybrid recognition method in this paper is 97%, which is better than the single recognition model. The average time taken by the wrist rehabilitation device on the seven tasks of lifting, grasping, undertaking, pulling, pushing, probing down and probing up is between 2.06 and 2.67 seconds. The output moments of the wrist and elbow positions were 17.1 and 11.6 N.m respectively for the human body-worn wrist joint rehabilitation device with 50N driving force output, and the joint output moments decreased significantly, and the joint comfort of the human body was improved greatly.

Keywords: intelligent flexible device, wrist rehabilitation, joint moment, fuzzy-PI dual-mode control

1. Introduction

The wrist joint is less covered by muscle tissue, which is one of the common obstacles in the case of human activity or strain, and the stage of rehabilitation is long [1-2]. The traditional methods of wrist rehabilitation are mainly physical therapy, medication and surgery, which can relieve patients' pain and promote the recovery of joint function to a certain extent [3-5]. However, traditional methods have problems such as long treatment period and unstable effect [6]. Moreover, most of the places for prevention, treatment and postoperative rehabilitation of wrist and related injuries are concentrated

✉ Corresponding author.
E-mail address: 19982089416@163.com (Y. Hu).
Received 22 March 2024; Revised 05 June 2024; Accepted 10 December 2024; Published Online 16 April 2025.
DOI: 10.61091/jcmcc127b-431

in different levels of medical institutions, which creates great pressure on the cost of patient treatment, rational utilization of medical resources and social economy [7-9].

With the continuous development of science and technology, smart wearable devices, as emerging health treatment tools, have been more widely used in home rehabilitation, community rehabilitation and basic treatment in Internet hospitals, gradually showing their unique advantages in the field of rehabilitation [10-12]. Under this basic condition, it is of great significance to combine different flexible sensors with the new form of remote rehabilitation training to design a wrist rehabilitation device that integrates wearable equipment and rehabilitation training [13-15]. Applying this device to the validation and practice of remote wrist rehabilitation training, the rehabilitation resources can be utilized to a greater extent, and the goal of wrist rehabilitation can be accomplished with low cost and high efficiency [16-17].

The article analyzes the principle of flexible wearable devices and constructs a skeletal muscle-based joint moment estimation model to calculate the joint moment during elbow and wrist movements. Then the flexible pneumatic wrist joint system is designed, and the fuzzy-PI dual-mode control strategy is used to complete the behavioral control of the intelligent rehabilitation device, so as to construct the wrist joint intelligent flexible rehabilitation device. Explore the performance of this wrist joint intelligent flexible rehabilitation equipment, after analyzing the velocity response characteristics and motor vibration of this rehabilitation equipment, the hybrid recognition method used in this paper is compared with the single recognition model for the action recognition effect. The wrist intelligent flexible rehabilitation device is utilized to train passive and active rehabilitation characteristics and test the bending angle range of the device. Finally, the actual usability and comfort of the device is analyzed.

2. Design program for wrist rehabilitation equipment

2.1. Principles and Classification of Flexible Wearable Devices

The core component of flexible wearable devices is flexible sensors [18], the principle of flexible sensors is to convert external deformation signals into electrical signals, according to the signal conversion method can be flexible wearable devices can be divided into piezoresistive, capacitive, piezoelectric. The signal conversion mechanism of piezoresistive is to convert the deformation signal into a change of resistance: according to the formula of resistance:

$$R = \rho L / S \tag{1}$$

where ρ is the resistivity, L is the resistive length, and S is the cross-sectional area. When the device deformation, L, S change caused by resistance change. Piezoresistive has the advantage of high sensitivity, simple preparation process, the disadvantage of signal hysteresis, accuracy is affected by temperature, commonly used in large-scale motion monitoring, such as joint activity. Capacitive type consists of parallel plate capacitors, and its capacitance is calculated by the formula:

$$C = \varepsilon A / d \tag{2}$$

where ε is the dielectric constant, A is the area of the parallel plates and d is the distance between the two plates. When the device deformation A, d changes in capacitance changes. The advantages of capacitive type are high accuracy, wide monitoring range, the disadvantage is susceptible to external interference, often used for fine motion monitoring, such as swallowing, pronunciation of the vocal folds vibration. Piezoelectric by the piezoelectric effect of the material composition, when subjected to external pressure, the material of the internal electron migration to the two levels, the formation of a certain voltage with the internal electric field, the advantage is able to make a rapid response to the strain, suitable for monitoring dynamic changes in the signal, such as heart rate, respiration, etc., the disadvantage is that the strain is worse than the rest of the two, wearable comfort is poor. The three different signal conversion mechanisms for flexible wearable devices are shown in Figure 1.

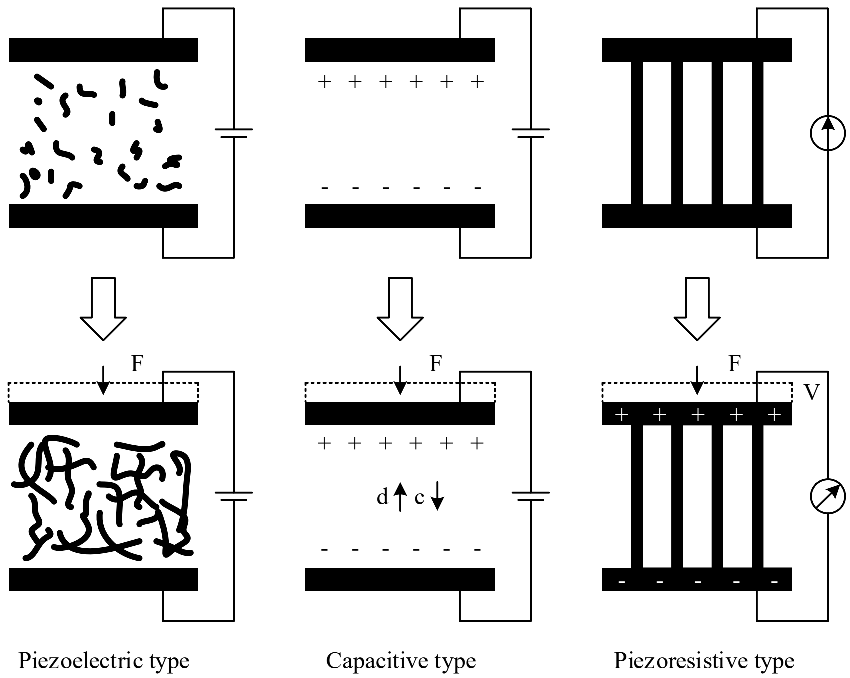

Fig. 1. Three different signal conversion mechanisms for flexible wearable devices

2.2. Elbow-wrist joint moment estimation

2.2.1. Joint moment estimation based on skeletal muscle modeling. When a muscle is activated, it will contract in different activation modes thus generating muscle contraction force. Therefore, this section first investigates the process of muscle contraction dynamics to realize the calculation of muscle force during exercise. Regarding the calculation of muscle force, there are two most representative muscle mechanics models: the Hill muscle model and the Huxley model, which is a one-dimensional model and does not take into account the effect of neural instructions on muscle contraction. Therefore, the Huxley model is seldom used in skeletal muscle modeling.The Hill muscle model, which takes muscle activation as an input [19], explains the physical and physiological properties of muscle contraction, and is widely used in muscle force calculations in skeletal muscle modeling. Therefore, in this paper, the Hill muscle model is selected to study the muscle contraction dynamics.The Hill muscle model is shown in Fig. 2.

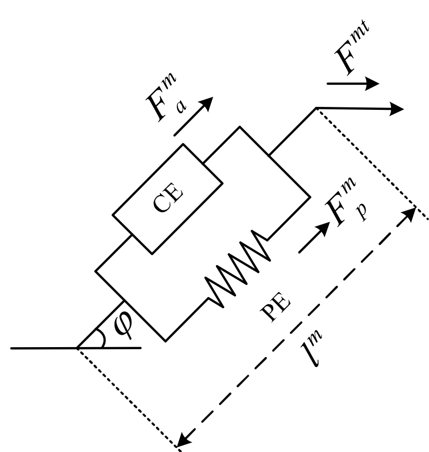

Fig. 2. Hill muscle model

The Hill model considers tendons and muscle fibers to be tandem structures, while muscle fibers consist of two main parts: the contractile element that generates the active contractile force F_a^m and the passive element that generates the passive contractile force F_p^m, which are parallel structures. As can be seen from Fig. 2, the relationship between the total muscle contraction force F, the tendon end force F^{mt}, and the contraction force F^m produced by the muscle fibers that the muscle exhibits externally is:

$$F = F^{mt} = F^m \cos\varphi \tag{3}$$

where φ is the angle between the muscle fiber and the tendon, called the pinnation angle. In general, the range of variation in the pinnation angle of a muscle is small and can be regarded as a fixed constant value.

The muscle fiber contraction force can be expressed as:

$$F^m = (f_a(l) \cdot f_a(v) \cdot a + f_p(l)) \cdot F_{\max}^m \tag{4}$$

$$l = \frac{l^m}{l_o^m} \tag{5}$$

$$v = \frac{v^m}{v_{\max}^m} \tag{6}$$

where, $F_{\max}^m$ is the maximum isometric muscle contraction force, a is the muscle activation. l is the normalized muscle fiber length, l^m is the varying muscle fiber length, and l_O^m indicates the optimal muscle fiber length. v is the normalized muscle fiber contraction velocity, v^m indicates the varying muscle fiber contraction velocity, and $v_{\max}^m$ indicates the maximum muscle fiber contraction velocity. $f_a(l)$ denotes the relationship between the active contraction force of myofibers and the normalized myofiber length, $f_a(v)$ denotes the relationship between the active contraction force and the contraction velocity of myofibers, and $f_p(l)$ denotes the relationship between the passive contraction force and the length of myofibers. These three relationships are expressed by the formula:

$$f_a(l) = e^{-2(l-1)^2} \tag{7}$$

$$f_a(v) = \begin{cases} \dfrac{1+v}{1-4v}, & v \le 0 \\ \dfrac{0.8+18v}{0.8+10v}, & v > 0 \end{cases} \tag{8}$$

$$f_p(l) = \frac{e^{4(l-1)/0.6} - 1}{e^4 - 1} \tag{9}$$

Based on the above analysis, assuming that the values of $F_{\max}^m$, l_O^m, and $v_{\max}^m$, which are constant physiological parameters, are known, the magnitude of the muscle contraction force can be calculated by Eq. (4) by obtaining the value of the muscle fiber contraction length l^m, as well as the muscle fiber contraction velocity v^m.

After obtaining the muscle force and the force arm of each muscle relative to the joint, then the joint moment can be calculated by Equation (10):

$$T = \sum_{i=1}^{6} (F_{flex.i} - F_{ext.i}) \cdot r_i \tag{10}$$

wherein $F_{flex.i}$ denotes a muscle force calculated from an activation degree of the muscle corresponding to the flexion movement portion, $F_{ext.i}$ denotes a muscle force calculated from an activation degree of the muscle corresponding to the extension movement process. r_i denotes the force arm of the muscle relative to the joint. When the elbow joint moment is calculated, r_i represents the force arm of the muscle relative to the elbow joint. When calculating the wrist joint moment, r_i represents the force arm of the muscle relative to the wrist joint.

2.2.2. Calculation of reference joint moments. In this section, the inverse dynamics of elbow and wrist flexion and extension movements in the sagittal plane will be modeled, and then the estimated joint moments obtained from the forward dynamics will be compared and analyzed with those obtained from the inverse dynamics.

When analyzing the human motion from the perspective of inverse dynamics, it is usually necessary to simplify the human body into a rigid body model. The simplified rigid body model of the human upper extremity is shown in Figure 3.

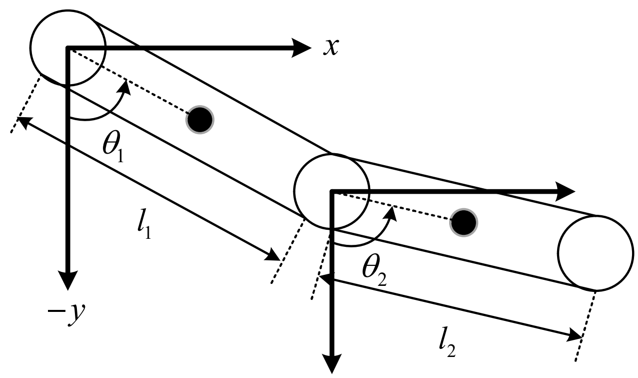

Fig. 3. Simplified rigid body model

The Lagrangian method is used to analyze the inverse dynamics without converting the coordinate system, and the solution process is concise and clear, so the Lagrangian method is chosen to analyze the upper limb dynamics problem in this paper. The Lagrange method starts from the energy perspective of the system and solves the dynamics problem through the Lagrange equation. The general form of Lagrange equation is:

$$F_i = \frac{d}{dt}\left(\frac{\partial L}{\partial \dot{q}_i}\right) - \frac{\partial L}{\partial q_i} \tag{11}$$

where F_i is the generalized force, q_i is the generalized coordinate, and L is called the Lagrangian function, which is the difference between the kinetic and potential energy of the system. In Fig. 3, the center of rotation of the elbow joint is taken as the origin of the coordinate system, l_1 denotes the length of the forearm, l_2 denotes the length of the hand (the palm and the fingers are considered as a whole in the study of this paper), and d_1 is used to denote the distance from the center of mass of the forearm to the center of the elbow joint, and d_2 denotes the distance from the center of mass of the hand to the center of the wrist joint, and θ_1 and θ_2 denote the two generalized coordinates, respectively. The masses of the forearm and hand are m_1 and m_2, respectively, and the centers of mass of the forearm and hand are C_1 and C_2, respectively, and their coordinates are (x_1, y_1) and (x_2, y_2), respectively:

$$\begin{cases} x_1 = d_1 \sin\theta_1 \\ y_1 = -d_1 \cos\theta_1 \end{cases} \tag{12}$$

$$\begin{cases} x_2 = l_1 \sin\theta_1 + d_2 \sin\theta_2 \\ y_2 = -l_1 \cos\theta_1 - d_2 \cos\theta_2 \end{cases} \tag{13}$$

From (12) and (13), we can obtain the change in the coordinates of the center of mass position, and the equations of motion of the center of mass can be obtained by taking the derivative of time:

$$\begin{cases} \dot{x}_1 = d_1 \cos\theta_1 \cdot \dot{\theta}_1 \\ \dot{y}_1 = d_1 \sin\theta_1 \cdot \dot{\theta}_1 \end{cases} \tag{14}$$

$$\begin{cases} \dot{x}_2 = l_1 \cos\theta_1 \cdot \dot{\theta}_1 + d_2 \cos\theta_2 \cdot \dot{\theta}_2 \\ \dot{y}_2 = l_1 \sin\theta_1 \cdot \dot{\theta}_1 + d_2 \sin\theta_2 \cdot \dot{\theta}_2 \end{cases} \tag{15}$$

Combining equations (14) and (15), the velocity of motion of the two centers of mass can be found to be:

$$v_1 = \sqrt{\dot{x}_1^2 + \dot{y}_1^2} = d_1 \dot{\theta}_1 \tag{16}$$

$$v_2 = \sqrt{\dot{x}_2^2 + \dot{y}_2^2} = \sqrt{(l_1\dot{\theta}_1)^2 + (d_2\dot{\theta}_2)^2 + 2 l_1 d_2 \dot{\theta}_1 \dot{\theta}_2 \cos(\theta_2 - \theta_1)} \tag{17}$$

From this, the kinetic energy of the system can be found $T = T_1 + T_2$, T_1 as the kinetic energy of the forearm and T_2 as the kinetic energy of the hand:

$$T_1 = \frac{1}{2} m_1 v_1^2 = \frac{1}{2} m_1 d_1^2 \dot{\theta}_1^2 \tag{18}$$

$$T_2 = \frac{1}{2} m_2 v_2^2 = \frac{1}{2} m_2 \left[(l_1\dot{\theta}_1)^2 + (d_2\dot{\theta}_2)^2 + 2 l_1 d_2 \dot{\theta}_1 \dot{\theta}_2 \cos(\theta_2 - \theta_1) \right] \tag{19}$$

After finding the kinetic energy of the system, it is also necessary to obtain the potential energy of the system $V = V_1 + V_2$. V_1 for the kinetic energy of the forearm and V_2 for the kinetic energy of the hand:

$$V_1 = -m_1 g d_1 \cos\theta_1 \tag{20}$$

$$V_2 = -m_2 g (l_1 \cos\theta_1 + d_2 \cos\theta_2) \tag{21}$$

Therefore, the Lagrangian function of the system can be obtained as:

$$\begin{aligned} L = T - V = {} & \frac{1}{2} m_1 d_1^2 \dot{\theta}_1^2 + \frac{1}{2} m_2 [(l_1\dot{\theta}_1)^2 + (d_2\dot{\theta}_2)^2 \\ & + 2 l_1 d_2 \dot{\theta}_1 \dot{\theta}_2 \cos(\theta_2 - \theta_1)] + m_1 g d_1 \cos\theta_1 \\ & + - m_2 g (l_1 \cos\theta_1 + d_2 \cos\theta_2) \end{aligned} \tag{22}$$

Based on the Lagrange equation, partial derivatives are obtained for $\dot{\theta}_1$, $\dot{\theta}_2$ and θ_1, θ_2, respectively:

$$\frac{\partial L}{\partial \dot{\theta}_1} = (m_1 d_1^2 + m_2 l_1^2)\dot{\theta}_1 + m_2 l_1 d_2 \dot{\theta}_2 \cos(\theta_2 - \theta_1) \tag{23}$$

$$\frac{\partial L}{\partial \dot{\theta}_2} = m_2 d_2^2 \dot{\theta}_2 + m_2 l_1 d_2 \dot{\theta}_1 \cos(\theta_2 - \theta_1) \tag{24}$$

$$\frac{\partial L}{\partial \theta_1} = -(m_1 g d_1 + m_2 g l_1)\sin\theta_1 + m_2 l_1 d_2 \dot{\theta}_1 \dot{\theta}_2 \sin(\theta_2 - \theta_1) \tag{25}$$

$$\frac{\partial L}{\partial \theta_2} = -m_2 g d_2 \sin\theta_2 - m_2 l_1 d_2 \dot{\theta}_1 \dot{\theta}_2 \sin(\theta_2 - \theta_1) \tag{26}$$

Then the derivation can be obtained:

$$\begin{aligned} \frac{d}{dt}\left(\frac{\partial L}{\partial \dot{\theta}_1}\right) &= (m_1 d_1^2 + m_2 l_1^2)\ddot{\theta}_1 + m_2 l_1 d_2 \ddot{\theta}_2 \cos(\theta_2 - \theta_1) \\ &\quad - m_2 l_1 d_2 \dot{\theta}_2^2 \sin(\theta_2 - \theta_1) + m_2 l_1 d_2 \dot{\theta}_1 \dot{\theta}_2 \sin(\theta_2 - \theta_1) \end{aligned} \tag{27}$$

$$\begin{aligned} \frac{d}{dt}\left(\frac{\partial L}{\partial \dot{\theta}_2}\right) &= m_2 {d_2}^2 \ddot{\theta}_2 + m_2 l_1 d_2 \ddot{\theta}_1 \cos(\theta_2 - \theta_1) \\ &\quad + m_2 l_1 d_2 \dot{\theta}_1^2 \sin(\theta_2 - \theta_1) - m_2 l_1 d_2 \dot{\theta}_1 \dot{\theta}_2 \sin(\theta_2 - \theta_1) \end{aligned} \tag{28}$$

Substituting into the Lagrange equation:

$$\begin{cases} T_e = \dfrac{d}{dt}\left(\dfrac{\partial L}{\partial \dot{\theta}_1}\right) - \dfrac{\partial L}{\partial \theta_1} \\ T_w = \dfrac{d}{dt}\left(\dfrac{\partial L}{\partial \dot{\theta}_2}\right) - \dfrac{\partial L}{\partial \theta_2} \end{cases} \tag{29}$$

As a result, the moments of the two joints can be obtained from the inverse dynamics calculation:

$$\begin{cases} T_e = (m_1 d_1^2 + m_2 l_1^2)\ddot{\theta}_1 + m_2 l_1 d_2 \ddot{\theta}_2 \cos(\theta_2 - \theta_1) \\ - m_2 l_1 d_2 \dot{\theta}_2^2 \sin(\theta_2 - \theta_1) + (m_1 g d_1 + m_2 g l_1)\sin\theta_1 \\ \quad T_w = m_2 {d_2}^2 \ddot{\theta}_2 + m_2 l_1 d_2 \ddot{\theta}_1 \cos(\theta_2 - \theta_1) \\ \quad + m_2 l_1 d_2 \dot{\theta}_1^2 \sin(\theta_2 - \theta_1) + m_2 g d_2 \sin\theta_2 \end{cases} \tag{30}$$

In Eq. (30), T_e represents the elbow joint moment and T_w represents the wrist joint moment. Eqs. m_1, m_2, l_1, d_1 and d_2 involved in Eqs. (30) are physical parameters of the human body, which can be estimated according to the national standard of inertia parameters of the human body. This standard establishes the binary regression equations of mass, center of mass position and height and weight of each body part of Chinese adults:

$$Y = B_0 + B_1 X_1 + B_2 X_2 \tag{31}$$

where, B_0 is the constant term of the binary regression equation, B_1 is the regression coefficient of weight and B_2 is the regression coefficient of height. X_1 and X_2 denote weight and height in kg and mm respectively.

2.3. *Flexible pneumatic wrist joint system design*

The overall system of the flexible pneumatic wrist joint is shown in Fig. 4, which includes three main parts: control system, data acquisition system and pneumatic actuation system.

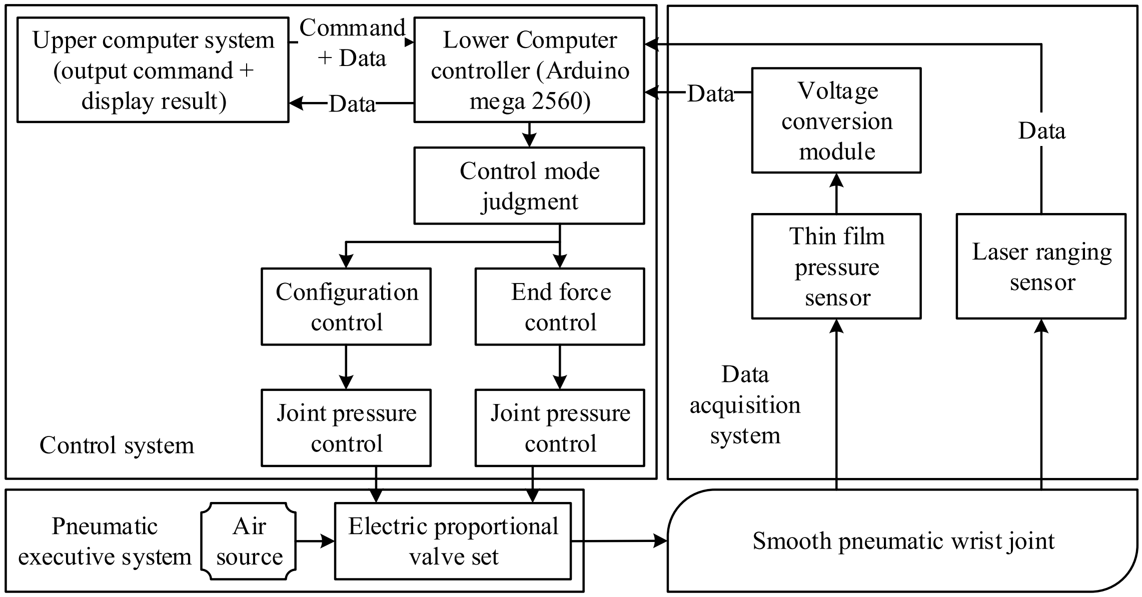

Fig. 4. The overall system of the flexible pneumatic wrist joint

The control system consists of an upper computer system and a lower computer controller. The lower computer center controller is used to receive the data information collected by the sensor and transmit it to the upper computer. The upper computer interface can display the data information and give commands to the lower computer. The data acquisition system mainly consists of laser range sensors and thin-film pressure sensors. The laser distance sensor can collect the height and position information of the flexible pneumatic wrist joint, and convert the information into digital signals to be transmitted to the lower computer center controller. Thin-film pressure sensor can collect flexible pneumatic wrist joint gripping force information, and convert the information into voltage signals. Through the voltage conversion module can be converted into analog signals and digital signals, and then pass the information to the lower computer center controller. The pneumatic actuation system mainly includes an air pump and an electrical proportional valve, which can provide pressure for the air cavity of the joint. Flexible pneumatic wrist joints need to be driven by the air cavity pressure to perform the action, the control system receives the feedback signal to the pneumatic actuator system to give instructions to adjust the joint air cavity pressure to achieve the target action.

As the gripping action process of the flexible pneumatic wrist joint can be divided into two phases, the control system performs two control modes for the action characteristics of the two phases: bit shape control and end force control, and the principle of the control mode of the flexible pneumatic wrist joint is shown in Figure 5. In the first stage, the flexible pneumatic wrist joint is not in contact with the target, the bit pattern control mode is executed to control the height of the end position, and the end height information is collected by the laser distance sensor and transmitted to the controller. In the second stage, the flexible pneumatic wrist joint contacts the target and generates contact force, executes the end force control mode, and the contact force information is collected by the thin-film pressure sensor and transmitted to the controller. The controller calculates the air cavity pressure of each joint based on the initial target value and feedback information relying on the control strategy, and transmits the control signal to the pneumatic actuator system to drive the flexible pneumatic wrist joint to execute the target action.

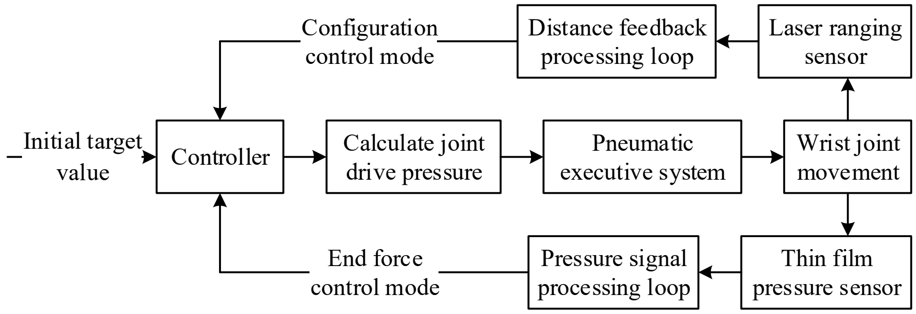

Fig. 5. The flexible pneumatic finger control pattern principle diagram

2.4. Flexible Pneumatic Wrist Control Strategy

2.4.1. Research on control strategies. The flexible pneumatic wrist joint grasps the target in two stages. In the first phase, the wrist joint does not make contact with the target. In the second stage, the wrist joint contacts the target and outputs the grasping force. According to the grasping characteristics of the flexible pneumatic wrist joint, two control strategies are used in this paper. The first stage adopts the position control strategy, and the second stage adopts the force control strategy.

First determine whether contact has occurred between the flexible pneumatic wrist joint and the target. The method of judging the contact is to refer to the return value of the thin-film pressure sensor, if it is greater than 0.1N, then it is judged as contacted, otherwise it is judged as not contacted. If there is no contact, the position control mode is used. If contact has been made, the force control mode is used.

In position control mode, firstly, the flexible pneumatic wrist joint is driven to lift to the highest position to prepare for grasping the target. When the target is within the grasping range, the laser distance sensor of the flexible pneumatic wrist joint is utilized to measure the distance between the end and the target, and the control algorithm is called to adjust the pressure of the air cavity of each joint to adjust the position of the end. Finally, when the flexible pneumatic wrist joint is in contact with the target, it is switched to the force control mode.

In the force control mode, first, the initial end force value of the flexible pneumatic wrist joint is set, and the thin-film pressure sensor is used to collect information. When the end force does not meet the set value, the control algorithm is called to adjust the pressure of the air cavity of each joint to adjust the end force output. Finally, when the end force collected by the sensor is equal to the given value, the air cavity pressure of each joint is maintained to maintain a stable gripping state.

2.4.2. Research on control methods. In this paper, the position control method and force control method of the flexible pneumatic wrist joint are studied according to the relevant methods in fuzzy control theory.

The position control of flexible pneumatic wrist joint adopts fuzzy-PI dual mode control [20], and the system structure is shown in Fig. 6. A selection switch is added to the control system and the switch threshold is set to 20%. The fuzzy controller is selected when the system deviation is greater than the threshold to obtain better dynamic performance. The PI controller is selected when the system deviation is less than the threshold value to achieve better steady state performance. The end height information $H(s)$ is collected by the laser range sensor, and the deviation value e is obtained by the difference between it and the target height $H_0(s)$. The deviation value e is inputted into the fuzzy-PI dual-mode controller to obtain the control parameters. According to the control parameters, the air cavity pressure of the three joints is calculated by combining with the theoretical model, and the pressure command is sent to the pneumatic actuator system. The height position of the end of the flexible pneumatic finger is adjusted by regulating the air cavity pressure of each joint through the electrical proportional valve.

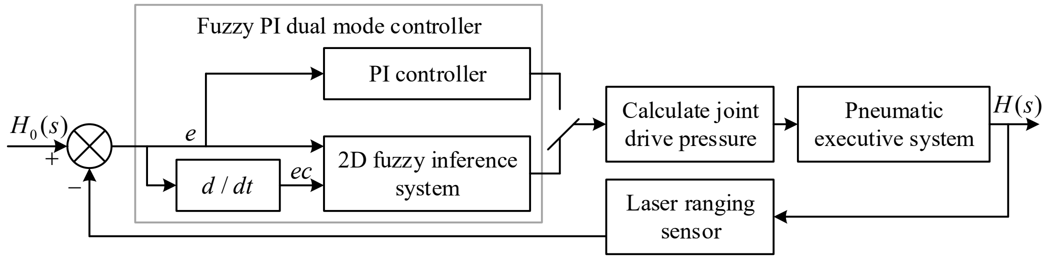

Fig. 6. Fuzzy-PI dual mode control system structure diagram

The PI controller utilizes proportional and integral regulation to process the deviation value e to obtain the control parameter u and send it to the controlled object [21]. By adjusting the proportional and integral constants K_p and K_i, the response speed and steady state performance of the system can be adjusted.

Fuzzy controllers are usually categorized into one-dimensional fuzzy controllers and two-dimensional fuzzy controllers. The two-dimensional fuzzy controller has more excellent performance by considering the effects of both the deviation value e and the rate of change of the deviation value ec. In this paper, the two-dimensional fuzzy controller is selected. The control parameter u is the output quantity, and K_e, K_{ec} and K_u are the quantization factors of deviation value e, deviation value change rate ec and control parameter u respectively. The performance of the controller can be adjusted by adjusting the quantization factor of the three parameters.

3. Performance test analysis of intelligent rehabilitation equipment

3.1. Velocity characteristics and motor vibration

Fuzzy-PI dual-mode control adjusts the traditional PID velocity loop control and improves the adaptive control ability of the system. In the wrist rehabilitation system, the traditional PID controller and fuzzy-PI dual-mode controller are used for the motion control of the main stepping motor of the wrist rehabilitation equipment, and the piezoelectric ceramic vibration sensors are used for detecting the vibration of the motor, and the velocity response characteristics are printed through the serial port, and with the help of the MATLAB drawing tool to observe the control effect of traditional PID and fuzzy-PI.

3.1.1. Velocity response characteristics. Under the passive training of the wrist joint, the speed of the first 5 seconds of the motor start-up phase is sampled at a sampling frequency of 100 Hz, and the speeds regulated by the traditional PID control and the fuzzy-PI bimodal control are outputted, and the output effect is shown in Fig. 7, in which the black solid line is the fuzzy-PI speed response curve and the red solid line is the traditional PID speed response curve.

It can be seen that the stepper motor system controlled by fuzzy-PI dual-mode controller has a faster response speed in the first 0.5 seconds of motor startup. In the acceleration phase from 0.5 seconds to 1.26 seconds, the acceleration process is smoother compared to the traditional PID control. In the speed maintenance phase from 1.26 seconds to 5 seconds, it has better stabilization characteristics, which can meet the patient's rehabilitation needs and improve the user experience of the wrist rehabilitation equipment.

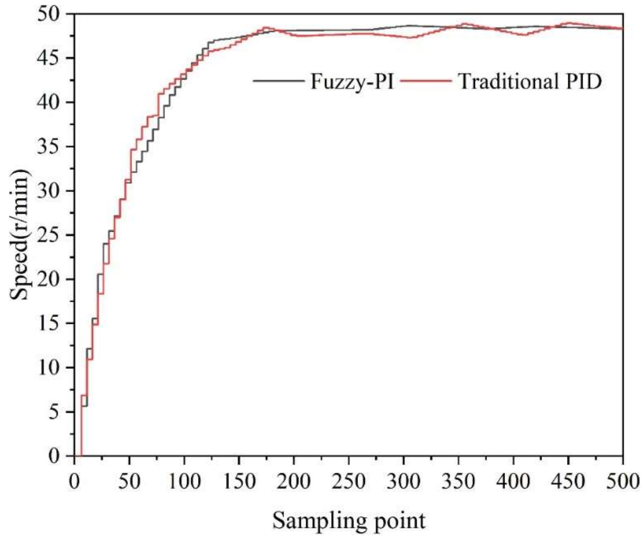

Fig. 7. Measured velocity response curve of traditional PID and fuzzy-PI

3.1.2. Motor vibration. This system uses piezoelectric ceramic vibration sensor to detect the motor vibration with a sampling frequency of 100Hz, and samples the vibration of the first 6 seconds of the motor startup phase under the passive training of the wrist joint, outputs the vibration sensor data through the serial port, and uses the MATLB drawing tool to show the motor vibration under the traditional PID and the fuzzy-PI bimodal control in the form of a two-dimensional coordinate graph, and vibration comparative The effect is shown in Fig. 8, where the red solid line corresponds to the motor vibration waveform under traditional PID control and the black solid line corresponds to the motor vibration waveform under fuzzy PID control.

Analyzing the test results, during the startup phase, the amplitude of motor vibration detected by the vibration sensor fluctuates up and down around 1835, and the vibration frequency is around 12Hz. The motor controlled by the traditional PID controller with fixed parameters, compared with the fuzzy-PI dual-mode controller, the amplitude of the former is about 2.5-3 times that of the latter, and it can be seen that the use of the fuzzy-PI dual-mode controller effectively reduces the vibration noise of the motor during the startup phase.

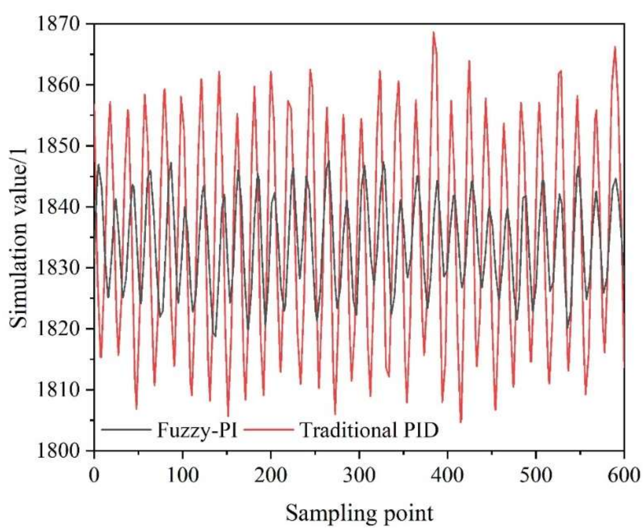

Fig. 8. Motor curve of traditional PID and fuzzy-PI

3.2. Motion Recognition Effect

This subsection tests the effectiveness of the conventional force-position control model, the EMG-aware model, and the hybrid recognition model of conventional force-position control and EMG-awareness used in this paper for classifying wrist movements.

3.2.1. Force Level Control Recognition Effects. The force position control model, mainly through the force sensor to collect the pressure information of the wrist area of the LLRR working in the active training mode, and according to the information on the patient's movement intention to recognize, control the LLRR to perform the corresponding action, improve the patient's participation in the rehabilitation training process.

In the experiment, five healthy subjects (No. A~E) were selected and had not performed strenuous exercise in the last three days, the subjects performed wrist palm flexion, dorsiflexion, internal retraction, abduction, internal turning, external turning movements in turn, the duration of each movement was not less than 3s, and after the equipment distinguished the movements, the interval between the switching of the movements in each session was not less than 5s, and each movement was repeated for five times for two rounds of the movement experiments, and two rounds of the movement experiments could be obtained by this method for each name 60 actions of each subject, a total of 300 actions of 5 subjects, the accuracy of action recognition was calculated, and the results are shown in Table 1.

It can be seen that the recognition accuracies of the six movements of palm flexion, dorsiflexion, adduction, abduction, inversion, and eversion were 0.92, 0.86, 0.90, 0.90, 0.92, 0.88, respectively, and the combined accuracy was 0.90. Among the four movements, the recognition rates of palm flexion and inversion reached 92%. Among the six groups of action recognition, the recognition rate of wrist dorsiflexion action is the lowest, only 86%. Analyzing the reason, due to the variability of the tester's wrist size, the position of the wrist force application and the placement position of the sensors in the testing of the testers A, B, and E are deviated, which makes the sensors not able to measure the force application of the wrist very well, and increases the error of the action recognition.

Table 1. Force bit control model action recognition results

Action	A	B	C	D	E	Overall
Palm bending	9	8	9	10	10	0.92
Handback bending	8	8	10	9	8	0.86
Inward contraction	9	10	9	8	9	0.90
Outward unfolding	9	10	9	9	8	0.90
Inward flipping	10	9	8	9	10	0.92
Outward flipping	9	9	8	10	8	0.88
Total	54	54	53	55	53	269
Accuracy	0.90	0.90	0.88	0.92	0.88	0.90

3.2.2. Myoelectric sensing knowledge of aliasing effects. In the experiment, the five healthy subjects in section 3.2.1 were still selected to perform the six movements of palmar flexion, dorsiflexion, adduction, abduction, inversion, and eversion in turn, and 20 sets of data were collected for each movement of each person, and 100 sets of data were collected for a single movement, totaling 600 sets of data, so as to obtain the original sEMG dataset, and to extract the eigenvalues of the six movements in the time and frequency domains to form a 10-dimensional eigenvector. Sixty sample data from each action dataset were randomly selected for model training, and the remaining 40 sample data were used for model testing.

According to manual experience, the SVM algorithm model hyperparameter C is set to take values between 2^{-5} and 2^{15}, and the gamma parameter is set to take values between 2^{-15} and 2^{3}, and all the combinations of C and gamma are traversed to find the most suitable C and gamma so that the trained model has the highest recognition rate. Due to the limitation of the collection conditions, the training sample dataset is small, and in order to find the optimal C and gamma and obtain a more accurate training model, the training samples are augmented by using five-fold cross-validation. The 200 sample data were randomly disrupted and 120 of them were selected for training, after which the integrated recognition rate was obtained. Radial basis kernel, Laplace kernel, and Sigmoid kernel were used to construct the SVM algorithm model for wrist movement classification respectively, and the measured results of movement classification under different kernel functions are shown in Table 2.

The analysis shows that among the three kernel functions for SVM algorithm modeling, the RBF kernel, Laplace kernel, and Sigmoid kernel are used for dorsiflexion, palmar flexion, and valgus classification with the highest recognition rate, respectively. Using sEMG for movement classification, the optimal recognition rates for the six movements of palm flexion, dorsiflexion, adduction, abduction, inversion, and eversion were 0.9125, 0.9250, 0.9250, 0.9375, 0.9000, 0.9750, respectively, and the combined recognition rate was 0.9292, which was higher than the combined accuracy of the force-position control model. The recognition accuracies of the six movements were relatively smooth, and in the recognition of the movements of the wrist joint, the use of the myoelectric perception model had a significantly better recognition effect than that of the force-position control model.

Table 2. Action identification results under different kernel functions

Action	RBF kernel	Laplacian kernel	Sigmoid kernel
Palm bending	0.8875	0.9125	0.8875
Handback bending	0.9250	0.8750	0.8875
Inward contraction	0.8750	0.8250	0.9250
Outward unfolding	0.9125	0.8125	0.9375
Inward flipping	0.8875	0.9000	0.9000
Outward flipping	0.9125	0.8250	0.9750

3.2.3. Mixed recognition effects. Experiment in the same 3.2.1 section and 3.2.2 section of the five healthy subjects, in turn, palm flexion, dorsiflexion, inward retraction, abduction, inward turning, outward turning action, each action duration of not less than 3s, the equipment to distinguish the action, the links of the action switching time interval of not less than 5s, each action is repeated five times, two rounds of action experiments, the use of hybrid recognition model of the action to prejudge the results of recognition are shown in Table 3.

Using the joint moment estimation action classification model, the recognition accuracies of the six actions of palmar flexion, dorsiflexion, adduction, abduction, inversion, and eversion were 0.98, 0.94, 0.98, 0.96, 0.98, 0.96, respectively, and the comprehensive accuracy reached 0.97. Compared with a single force-position control model, the six actions maintained a high recognition rate, and the recognition accuracies were relatively smooth due to the differences brought about by the The problems of low recognition rate and unstable recognition effect of the wrist joint action brought by the difference are also compensated. Comprehensive analysis can conclude that the designed hybrid recognition model can make up for the physical differences existing in the single model, and at the same time has a higher and more stable action classification effect, which meets the design requirements of the action classification of the lower limb rehabilitation system.

Table 3. Fuzzy-PI identification model

Action	A	B	C	D	E	Overall
Palm bending	9	10	10	10	10	0.98
Handback bending	9	10	9	9	10	0.94

Inward contraction	10	9	10	10	10	0.98
Outward unfolding	10	10	10	9	9	0.96
Inward flipping	10	9	10	10	10	0.98
Outward flipping	9	10	9	10	10	0.96
Total	57	58	58	58	59	290
Accuracy	0.95	0.97	0.97	0.97	0.98	0.97

3.3. Carpal Rehabilitation Tests

In order to verify the reliability of the structure and control system of the wrist rehabilitation equipment designed in this paper, this subsection builds an experimental platform of the wrist training equipment and carries out passive and active control experiments with healthy human hands.

After completing the construction of the experimental platform, in order to verify whether the designed wrist rehabilitation equipment can help patients realize the active and passive training of the wrist joint, this paper carries out passive rehabilitation training experiments and active rehabilitation training experiments with healthy human hands respectively, with the following experimental purposes:

1) To verify the reasonableness of the structural design of the wrist rehabilitation equipment, whether it can realize the flexion and extension training of the wrist joint, and to test the stability of the control system during the movement of the wrist rehabilitation equipment.

2) Verify whether the linear motor can be driven smoothly according to the preset program to realize the flexion and extension movement of the wrist joint when the wrist rehabilitation equipment carries out the passive rehabilitation training experiment.

3) Verify that when the wrist rehabilitation equipment performs active rehabilitation training experiments, the linear motor can move the push rod for a small period of time until the bending angle required by the training is reached when the wrist pressure detected by the thin-film pressure sensor reaches the preset threshold value.

3.3.1. Passive Rehabilitation Training Tests. In this experiment, four experimental subjects were selected for the passive rehabilitation training experiment. The experimental subjects were selected: two females a, b and two males c, d. The experimenters selected the passive rehabilitation training mode through the software of the upper computer, chose the low-speed training, and carried out the bending/extension rehabilitation training experiments on the fingers of the experimental subjects according to the predetermined program. The range of changes in the flexion angle of the wrist joint of the experimental subjects during the training process was recorded as shown in Table 4.

As can be seen from Table 4, in general, each experimental subject basically reached the set bending angle when performing wrist flexion/extension exercise, and there was no phenomenon that exceeded the threshold range during the training process.

Table 4. Wrist joint bending angle in passive training

	a	b	c	d
Training speed	Low speed	Low speed	Low speed	Low speed
Palm bending	0-55.16°	0-55.46°	0-55.42°	0-53.68°
Handback bending	0-50.12°	0-50.05°	0-51.36°	0-52.25°
Inward contraction	0-50.36°	0-51.52°	0-52.36°	0-51.41°
Outward unfolding	0-52.03°	0-53.64°	0-52.41°	0-50.62°
Inward flipping	0-51.68°	0-52.14°	0-50.85°	0-50.51°
Outward flipping	0-54.36°	0-51.95°	0-52.15°	0-50.45°

3.3.2. Active Rehabilitation Training Test. In the active rehabilitation training mode, the finger rehabilitation equipment is used to control the movement of the linear motor through the signal feedback from the membrane pressure sensor. When the detected fingertip pressure is greater than the pressure threshold, the linear motor moves. In this mode, the experimenter conducts active grasping training experiments. During this process, the bending angle of the index finger of the experimenter at five key time points was recorded as shown in Table 5.

From Table 5, it can be seen that under the active rehabilitation training mode, the wrist rehabilitation equipment can drive the experimental subject's wrist joint for grasping training. At the same time, the angle of wrist joint bending is within the safety range set by the program. Due to the individual differences between the experimental subjects, the wrist force output is different when making resistance resistance movement, so there is variability in the value of the bending angle at the same moment.

Table 5. Wrist joint bending angle in grab training

Time (s)	0	4	8	12	16	20
a	0	40.62	60.85	59.41	35.48	24.62
b	0	41.25	60.34	59.25	35.36	23.48
c	0	42.62	61.42	60.15	34.52	22.76
d	0	43.85	61.58	60.21	34.28	22.15

3.4. Device Availability Testing

Device usability testing is the process of testing the ease of use of a software interface. Its main purpose is to assess the user-friendliness of the software interface and to identify and resolve possible problems so as to improve the user experience and satisfaction. The role of device usability testing includes:

1) Discovering device problems: through testing, problems with the device can be discovered, such as unclear navigation structure, complex operation flow, etc., which helps to improve the device and enhance the user experience.

2) Determine the ease of use of the device: device usability testing can assess the ease of use and user experience of the device, and determine whether it can meet the needs and expectations of users.

3) Optimize the user experience: through the test results, make optimization of the user experience, improve the user satisfaction and use of the device.

4) Reduce user learning costs: Optimizing the design of the device can reduce the user's learning costs and improve user satisfaction and loyalty.

5) Improve the market competitiveness of the software: a quality user experience will make the device more competitive in the market, attract more users to use and improve the reputation and credibility of the device.

In this paper, 10 experimental subjects were selected to test the usability of the wrist rehabilitation equipment through Figma software, which designs the interaction flow of the equipment through the prototype setup function, and simulates the user's manipulation of the high-fidelity pages, components and buttons (clicking, dragging and hovering, etc.), and then sets up the corresponding interaction effects (bending, stretching, flipping effects, etc.). After the interaction logic is set up, the device can be tested for usability, for example, by analyzing the effectiveness and efficiency of the designed device through indicators such as task completion rate, completion time, and number of errors.

Through the usability test, the user's task completion rate, error rate, and task completion time when completing the tasks were measured, etc. All 10 subjects successfully completed the test tasks during the task test, with a completion rate of 100%, which verified the effectiveness of the device design.

The error rate of the device was tallied by testing the rehabilitation device on 7 tasks (lifting, grasping, undertaking, pulling, pushing, down probing, and up probing). Ten attempts were made for each task. The error rate statistics of the tasks in the usability test are shown in Table 6.

From the error rate data, the error rate of task 4 and task 5 is higher, both at 10%, while the error rate of other tasks is relatively low. Combined with the user's actual operation path, in the usability test of task 4, due to the low distinction between “pull” and “push”, it is easy to cause misoperation.

Table 6. Task error rate statistics in usability test

Task	1	2	3	4	5	6	7
Error number	0	0	0	1	1	0	0
Error rate	0	0	0	10%	10%	0	0

The statistics of the completion time of each task are shown in Table 7. In the case that each subject did not have prior contact with the wrist rehabilitation equipment, the data statistics of the average time for the completion of each task are more reasonable. Due to the differences in the subjects' knowledge of the rehabilitation equipment, their personal cognitive level, and their understanding of the equipment, when the operation steps of the test tasks become complex, the corresponding gap between the operation performance performance and the completion time is also larger relative to the tasks with simpler operations.

From Table 7, it can be found that the average time taken by the wrist rehabilitation device designed in this paper on the seven tasks (lifting, grasping, undertaking, pulling, pushing, probing down, probing up) is 2.42, 2.06, 2.58, 2.66, 2.67, 2.44, 2.63 seconds, respectively, which is not more than 3 seconds, so it can be seen that the wrist rehabilitation device designed in this paper is capable of completing the user's instructions in a shorter period of time.

Table 7. Complete task time statistics (s)

Task	1	2	3	4	5	6	7
Total	15.46	16.42	17.09	15.89	16.34	15.48	16.14
Mean	2.42	2.06	2.58	2.66	2.67	2.44	2.63
Maximum	5.36	5.87	6.03	5.29	6.41	5.32	5.59
Minimum	1.02	1.36	1.48	1.19	1.95	1.85	1.79
Absolute error	0.56	0.72	0.53	0.69	0.41	0.72	0.76

3.5. Evaluation of equipment comfort

Based on the final design of the flexible smart rehabilitation device for the wrist joint, the human comfort was simulated and analyzed by Siemens Tecnomatix Jack software. The designed rehabilitation device is connected to an elastic bandage on the surface of the human torso and finally worn on the human wrist position. Therefore analyzing the human comfort of the device during use requires presetting the specific physiological attributes of the user. The Advanced Scaling module of Siemens TecnomatixJack software is utilized to set the physiological parameters of the human body. The human body uses the wrist joint flexible intelligent rehabilitation equipment to complete the rehabilitation action of the specific joint force.

Since the wrist joint is often used in conjunction with the elbow joint for joint action, the driving force and the distance between the application of the force on the human wrist and elbow position during the operation of the device are collected. And according to the wrist, elbow position output torque to analyze the human body in the use of equipment in the process of specific comfort indicators. Rehabilitation equipment in the output of different driving force source and 25N driving force, the specific force generated by the human joints as shown in Figure 9, (a) and (b) are the different driving force source and 25N driving force under the human joints under the force condition.

When the human body wears the rehabilitation device with a driving force of 50N, the output moment at the wrist position is 17.1N.m, and the output moment at the elbow position is 11.6N.m. When the human body carries out the wrist exercise without wearing the rehabilitation device and with a load of 5KG, the output moment at the wrist joints is about 40N.m, and that at the elbow is about 18N.m. The human body wears the rehabilitation device to carry out the rehabilitation exercise without wearing the rehabilitation device and with a weight of 5KG, the output moment at the wrist joints is about 40N.m, and that at the elbow is about 18N.m. The human body wears the rehabilitation device to carry out the rehabilitation exercise without wearing the rehabilitation device.

When the human body wears the rehabilitation equipment for rehabilitation exercise, the output moment at the wrist as well as the elbow position decreases significantly. From the data, it can be seen that when the human body wears the wrist joint flexible intelligent rehabilitation equipment to carry out the relevant rehabilitation movements, the human body's joint comfort is greatly improved.

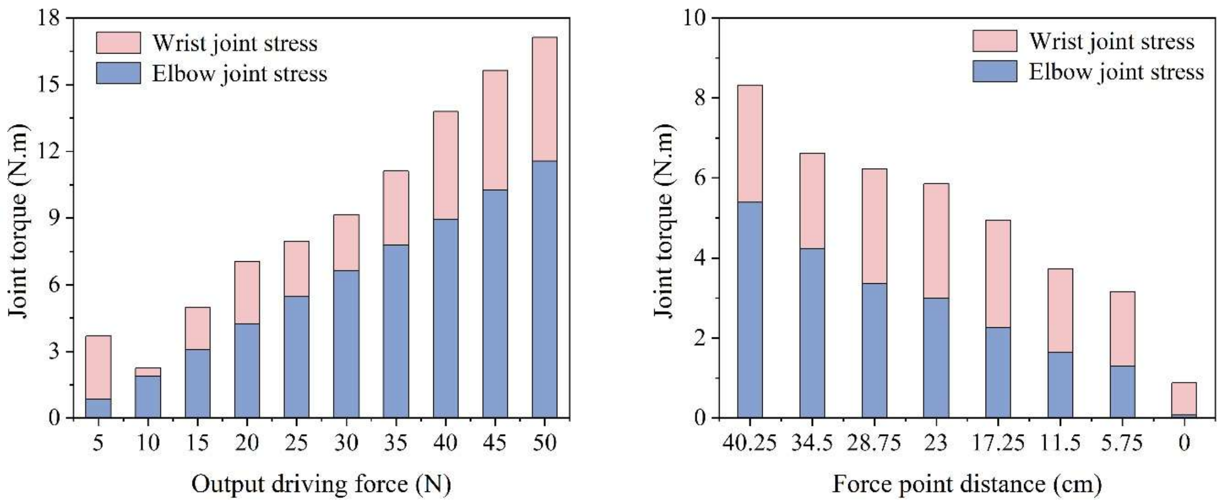

(a) Joint stress in different driving sources

(b) Joint stress in 25N driving sources

Fig. 9. Human joint stress

4. Conclusion

In this paper, we construct a skeletal muscle-based joint moment estimation model to calculate the elbow and wrist joint moments, combine the calculation results with the flexible wearable device to design a flexible pneumatic wrist joint system, and design a fuzzy-PI dual-mode control method to construct a flexible intelligent rehabilitation device for the wrist joint.

The fuzzy-PI dual-mode control method has a faster response speed than the traditional PID control strategy and can effectively reduce the vibration noise in the motor startup phase. In comparison with the single control model, the accuracy of the force-position control identification model, the myoelectric inductance knowledge identification model and the hybrid identification method in this paper are 92%, 93% and 97%, respectively. In both passive and active rehabilitation training of the wrist joint, the flexion angle of the wrist joint reached the set flexion angle. The average time taken by the wrist rehabilitation device on each of the seven tasks (lifting, grasping, undertaking, pulling, pushing, probing down, and probing up) did not exceed 3 seconds. When the human body wears the wrist rehabilitation equipment with a driving force of 50N, the output moments of the human wrist and elbow positions are 17.1 and 11.6N.m respectively, which are much smaller than the output moments of the wrist and elbow joints when the human body does not wear the rehabilitation equipment and is loaded with a weight of 5KG. The wrist joint flexible intelligent rehabilitation equipment has a greater improvement on the joint comfort of human body.

References

[1] Herde, B., & Stroia, K. A. (2018). Wrist and hand rehabilitation. Tennis Medicine: A Complete Guide to Evaluation, Treatment, and Rehabilitation, 327-357.

[2] Silva[1], B., Amorim[1], A. R., Leiras[1], V., Seabra[1], E., Silva[1], L. F., Braga, A. C., & Viana, R. (2021). for Wrist Rehabilitation in Adults and Young. Innovations in Mechatronics Engineering, 129.

[3] Zhang, L., Yu, Z., Su, P., Li, J., & Ge, R. (2024). Design of a parallel wrist rehabilitation robot and analysis of physiological effect on training. IEEE/ASME Transactions on Mechatronics, 29(5), 3401-3414.

[4] Wang, Y., & Xu, Q. (2019, July). Design of a new wrist rehabilitation robot based on soft fluidic muscle. In 2019 IEEE/ASME International Conference on Advanced Intelligent Mechatronics (AIM) (pp. 595-600). IEEE.

[5] Ballantyne, R., & Rea, P. M. (2019). A game changer:'the use of digital technologies in the management of upper limb rehabilitation'. Biomedical Visualisation: Volume 5, 117-147.

[6] Abdallah, I. B., Bouteraa, Y., & Rekik, C. (2016, December). Web-based robot control for wrist telerehabilitation. In 2016 4th International Conference on Control Engineering & Information Technology (CEIT) (pp. 1-6). IEEE.

[7] Xu, D., Zhang, M., Xu, H., Fu, J., Li, X., & Xie, S. Q. (2019). Interactive compliance control of a wrist rehabilitation device (WReD) with enhanced training safety. Journal of healthcare engineering, 2019(1), 6537848.

[8] Ríos Rincón, A. M., Guptill, C., Liubaoerjijin, Y., Figeys, M., Koubasi, F., Gregson, G., & Miguel Cruz, A. (2025). Effectiveness of a New Device for Hand, Wrist, and Forearm Rehabilitation: Feasibility Randomized Controlled Trial. JMIR Rehabilitation and Assistive Technologies, 12, e62809.

[9] Panny, M., Mayr, A., Nagiller, M., & Kim, Y. (2020). A domestic robotic rehabilitation device for assessment of wrist function for outpatients. Journal of Rehabilitation and Assistive Technologies Engineering, 7, 2055668320961233.

[10] Zhang, L., Li, J., Cui, Y., Dong, M., Fang, B., & Zhang, P. (2020). Design and performance analysis of a parallel wrist rehabilitation robot (PWRR). Robotics and Autonomous Systems, 125, 103390.

[11] Seabra, E., Silva, L. F., Ferreira, R., & Leiras, V. (2018, June). Design, development and construction of a new medical wrist rehabilitation device: A project review. In International Conference on Innovation, Engineering and Entrepreneurship (pp. 199-205). Cham: Springer International Publishing.

[12] Petre, I., Deaconescu, A., Sarbu, F., Deaconescu, T., Sârbu, I. P. A. D. F., & Deaconescu, T. (2018). Pneumatic muscle actuated wrist rehabilitation equipment based on the fin ray principle. Stroj. Vestn. J. Mech. Eng, 64, 383-392.

[13] Filip, O., Deaconescu, A., & Deaconescu, T. (2021). Mechanical Design of a Bioinspired Compliant Robotic Wrist Rehabilitation Equipment. Applied Sciences, 11(3), 1246.

[14] Tang, D., & Gao, Y. (2018). Recent Patents on Wrist Rehabilitation Equipment. Recent Patents on Mechanical Engineering, 11(2), 91-99.

[15] Garcia, G. F., Gonçalves, R. S., & Carbone, G. (2024). A review of wrist rehabilitation robots and highlights needed for new devices. Machines, 12(5), 315.

[16] Hussain, S., Jamwal, P. K., Van Vliet, P., & Ghayesh, M. H. (2020). State-of-the-art robotic devices for wrist rehabilitation: Design and control aspects. IEEE Transactions on human-machine systems, 50(5), 361-372.

[17] Amali, L. Y., & Batan, I. M. L. (2020). Design of a Patient Wrist Rehabilitation Device with Servo Motor Drive. JMES The International Journal of Mechanical Engineering and Sciences, 4(2), 77-86.

[18] Xia Du, Xiaomin Zhang, Zhuang Zhao, Youjie Rong, Pengdi Cui & Xiaobo Huang. (2024). DLP Printing Eutectic Gels Crosslinked by Dopamine-Grafted Nano-Cellulose for Flexible Wearable Devices. Journal of Polymer Science(4),998-1009.

[19] Ayda Okan,Ulviye Bunyatova & Mustafa Dogan. (2024). The Innovative Algorithm of the Hill Muscle Model for the Biceps Brachii Muscle in the Sagittal Plane. Sensors & Transducers(2),91-96.

[20] Salam Ibrahim Khather,Muhammed Abduljaleel Ibrahim & Mustafa Hussein Ibrahim. (2023). Dual fuzzy logic PID controller based regulating of dc motor speed control with optimization using Harmony Search algorithm. Eastern-European Journal of Enterprise Technologies(8),6-14.

[21] Jagajyoti Panda,Sanjukta Chakraborty & Samit Ray Chaudhuri. (2025). Experimental evaluation of a servomechanism-based PI controller for seismic response control in smart base-isolated steel building. Journal of Constructional Steel Research109349-109349.